BIOTROPIA ISSN: 0215-6334 | e-ISSN: 1907-770X
The Southeast Asian Journal of Tropical Biology

Vol. 33 No. 2, 2026: 266 - 277
DOI: 10.11598/btb.2026.33.2.2783

Research Paper

# UNCOVERING GENETIC PATTERNS OF THE BARRED MUDSKIPPER ALONG THE WEST COAST OF BENGKULU USING THE *COI* GENE

**Fanni Khoirillah[1], Zuliyati Rohmah[2], Rury Eprilurahman[3], And Tuty Arisuryanti[1*]**

[1]Laboratory of Genetics and Breeding, Faculty of Biology, Gadjah Mada University, Yogyakarta 55281, Indonesia
[2]Laboratory of Animal Structure and Development, Faculty of Biology, Gadjah Mada University, Yogyakarta 55281, Indonesia
[3]Laboratory of Animal Systematics, Faculty of Biology, Gadjah Mada University, Yogyakarta 55281, Indonesia

## ARTICLE HIGLIGHTS

- First genetic baseline for mudskipper in western Sumatra
- One shared lineage links Bengkulu to southern Java
- High connectivity along an open, shallow coastline
- Coastal tides and currents shape genetic patterns
- Findings support regional scale conservation planning

**Article Information**

Received : 29 January 2026
Revised : 26 February 2026
Accepted : 27 February 2026
Available Online : 8 May 2026

***Corresponding author, e-mail:**
tuty-arisuryanti@ugm.ac.id

Copyright (c) 2026@author(s).

## ABSTRACT

The barred mudskipper, *Periophthalmus argentilineatus*, is an amphibious gobiid fish that exhibits fully terrestrial behavior during low tides. Previous research has suggested the presence of cryptic species within this taxon, complicating species identification due to highly similar morphological traits. Despite its ecological importance in intertidal ecosystems, information on the genetic variation and population structure of *P. argentilineatus* in Sumatra remains limited, and no such data have been reported from the West Coast of Bengkulu. Therefore, this study aimed to assess the genetic diversity and population structure of *P. argentilineatus* along this coastline using the mitochondrial *COI* gene. A total of 30 individuals were collected from three locations, i.e., Air Hitam Coast, Baai Mangrove Forest, and Teluk Sepang Coast. The *COI* gene was amplified (approximately 660 bp), and a final aligned fragment of 630 bp was used for genetic analyses. Phylogenetic reconstruction placed all Bengkulu samples within a single lineage corresponding to Clade C previously reported from southern Java. Clades A and B were not detected in the study area. Genetic distances among individuals ranged from 0.00 – 0.80%, indicating close relatedness within this lineage. Sequence analysis identified nine variable sites, including two parsimony-informative positions, resulting in nine haplotypes. Haplotype diversity was moderate (Hd = 0.708), whereas nucleotide diversity was low ($\pi$ = 0.00182). Negative Tajima's D values suggest recent demographic expansion or ongoing connectivity among populations. AMOVA and Fst analyses indicated low or undetectable genetic differentiation among sampling sites, consistent with substantial gene flow along the coastline. These findings establish a baseline genetic reference for *P. argentilineatus* in Bengkulu and contribute to understanding regional population connectivity along the western Indonesian coastline.

**Keywords**: *COI* gene, genetic diversity, haplotype variation, *Periophthalmus argentilineatus*, population structure

## INTRODUCTION

Mudskippers (family Oxudercidae) are widely distributed amphibious gobies inhabiting tropical and subtropical intertidal zones from West Africa to the Pacific Ocean (Murdy 1989; Thacker 2003). Barred mudskipper, *Periophthalmus argentilineatus*, one of the most common species, occupies mangrove forests and muddy coastal plains and exhibits unique morphological and behavioural adaptations that allow it to forage and move on land during low tide (Kutschera *et al.* 2013; Sunarni *et al.* 2016). In several coastal regions, this species serves not only as a local food source but also as a bioindicator of environmental health (Abiaobo *et al.* 2021).

Recent molecular studies across Indonesia have revealed substantial genetic divergence within populations of *P. argentilineatus*, suggesting

the presence of cryptic species that are not distinguishable through morphology alone. *COI*-based DNA barcoding detected deep genetic breaks in populations from the southern coast of Java, for example: 5.96% in Bantul (Aji & Arisuryanti 2021) and 2.41 – 6.12% across wider southern Java (Arisuryanti *et al.* 2024). High divergence has also been reported using mitochondrial and nuclear markers, including *D-loop*, *16S* rDNA, and *RAG-1* (Polgar *et al.* 2014), while evidence of cryptic diversity has been documented in related genera such as *Boleophthalmus* (Shabrina *et al.* 2024). These findings highlight the taxonomic complexity of mudskippers and underscore the importance of mitochondrial *COI* as a global standard marker for species identification (Lv 2014).

While research on cryptic species has expanded, studies examining intraspecific genetic variation and population structure of *P. argentilineatus* remain limited, particularly in Sumatra. Existing genetic data reveal high haplotype and nucleotide diversity in Java and NTB—18 haplotypes with Hd = 0.884 and $\pi$ = 0.03223 in southern Java (Arisuryanti *et al.* 2024), and 10 haplotypes with 42 polymorphic sites in combined populations from NTB and western Java (Rha'ifa *et al.* 2021). However, no genetic information is available for populations inhabiting the West Coast of Bengkulu, despite its extensive mangrove ecosystems and ecological significance.

## MATERIALS AND METHODS

### Sample Collection, DNA Extraction, *COI* Amplification, and Sequencing

A total of 30 *Periophthalmus argentilineatus* individuals were collected from three coastal localities along the West Coast of Bengkulu: Air Hitam Coast (PAH: 3°45'16.34" S, 102°15'31.07" E), the Bai Mangrove Forest (PB: 3°53'37.60" S, 102°18'28.84" E), and Teluk Sepang Coast (PTS: 3°56'27.67" S, 102°16'44.40" E) (Fig. 1).

Prior to tissue sampling, all specimens were morphologically identified following diagnostic characters described by Murdy (1989). Identification was based on external morphological features, including body coloration patterns, the presence and characteristics of the lateral stripe, fin morphology, and overall body proportions. Each specimen was photographed in situ for documentation before tissue collection. This preliminary identification ensured taxonomic accuracy prior to molecular analysis (Fig. 2).

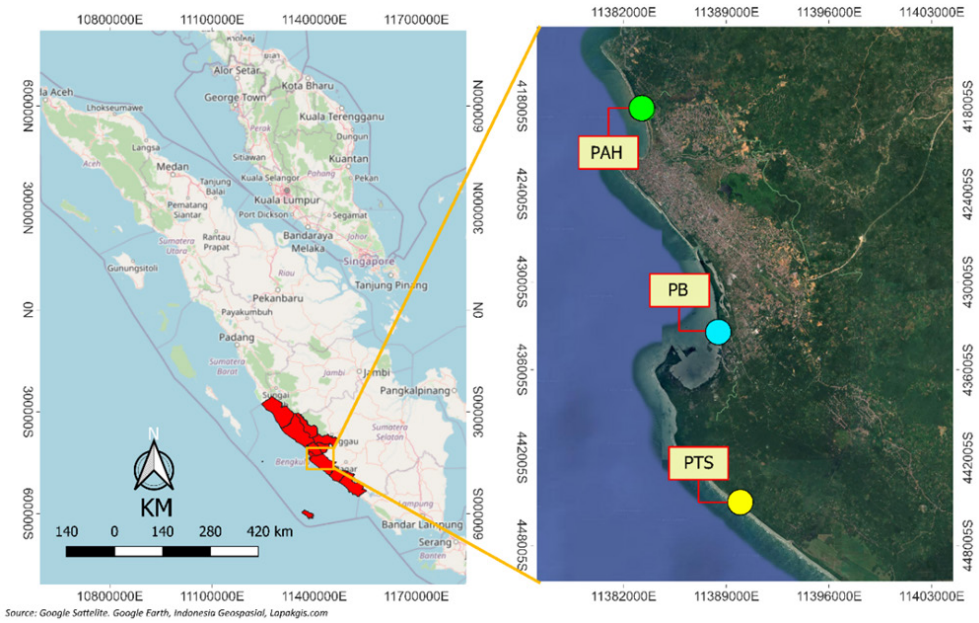


Figure 1 Three sampling sites of *P. argentilineatus* along the West Coast of Bengkulu

Notes: PB = Baai Mangrove Forest; PAH = Air Hitam Coast; PTS= Teluk Sepang Coast.

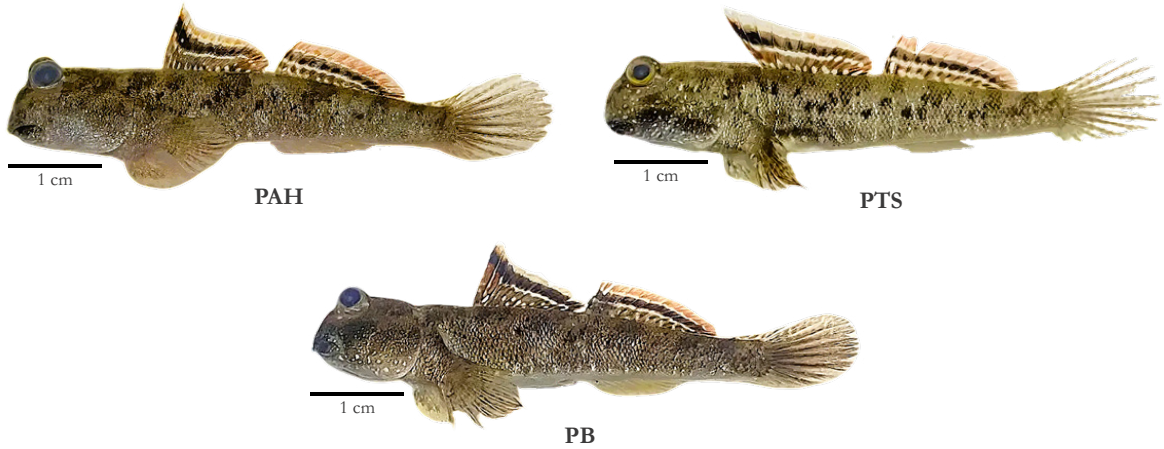


Figure 2 Morphology of *P. argentilineatus* specimens sampled from each study site
Notes: PAH = Air Hitam Coast; PTS= Teluk Sepang Coast; PB = Baai Mangrove Forest. Scale bar = 1 cm.

Approximately 50 – 100 mg of muscle tissue was dissected from the muscle near the pectoral fin using sterilized scissors, placed in 1.5-mL tubes, preserved in 99% ethanol on-site, and stored at –20 °C upon arrival in the laboratory. All procedures were reviewed and approved by the Animal Ethics Committee of the Faculty of Veterinary Medicine, Universitas Gadjah Mada, document number 37/EC-FKH/int./2025 dated 19 May 2025.

Genomic DNA was extracted from muscle tissue using the DNeasy Blood and Tissue Kit (QIAGEN, Valencia, CA, USA) following the manufacturer's protocol. A fragment of the mitochondrial *COI* gene was amplified using the universal fish primers **FishF2** (5'-TCGACTAATCATAAAGATATCGGCAC-3') and **FishR2** (5'-ACTTCAGGGTGACCGAAGAATCAGAA-3') (Ward *et al.* 2005).

PCR reactions were performed using the MyTaq HS Red Mix kit (Bioline) in 25 µL volumes containing 10 – 100 ng of template DNA, 12.5 µL MyTaq HS Red Mix, 1 mM $MgCl_2$, 0.6 µM of each primer, and nuclease-free water. Negative controls lacking DNA template were included to verify the absence of contamination. Amplifications followed cycling conditions modified from Arisuryanti *et al.* (2020). PCR products were separated on 1% agarose gels in TAE buffer, stained with FluoroSafe, and visualized under UV illumination. Purified amplicons were submitted to LPPT-UGM for bi-directional sequencing using BigDye Terminator chemistry (Applied Biosystems) on an Illumina 3500 Genetic Analyzer.

## Genetic Analyses

Raw chromatograms were edited and assembled using GeneStudio Pro in conjunction with EditSeq and SeqMan (DNASTAR, Madison, USA). Bi-directional reads were inspected manually to resolve ambiguous bases and detect potential stop codons. Edited sequences were exported in FASTA format via Mesquite v3.5 (Maddison & Maddison 2018). Alignment was performed using OPAL in Mesquite and verified with ClustalW implemented in MEGA11 (Tamura *et al.* 2021). A total of 30 *COI* sequences were analyzed to assess intraspecific genetic variation and phylogenetic relationships. Nucleotide composition and GC content were estimated using DNASTAR and validated with DnaSP v6 (Rozas *et al.* 2017). Measures of genetic diversity including the number of haplotypes, polymorphic sites, haplotype diversity (Hd), and nucleotide diversity ($\pi$) were calculated in DnaSP v6.

Genetic distances were computed using the Kimura 2-Parameter (K2P) model, and a Neighbor-Joining (NJ) tree was reconstructed with 1,000 bootstrap replicates following the standard DNA barcoding framework (Hebert *et al.* 2003). Bayesian phylogenetic inference was conducted in BEAST v1.10 (Suchard *et al.* 2018) using the best-fit substitution model identified through the Akaike Information Criterion (AIC) in jModelTest v2.1.10 (Darriba *et al.* 2012). Two independent MCMC runs were executed for 10 million generations with sampling every 1,000 generations; a 25% burn-in was applied prior to constructing consensus trees, which were visualized in FigTree v1.4.4 (Rambaut 2019).

Previously published *COI* sequences of *P. argentilineatus* (accession numbers KU692746, MZ606686, MZ606685, OQ804360, OQ804361, PP593624, PP593608) were included for comparative analyses, while *P. novemradiatus* (KU692765) was used as an outgroup. Patterns of haplotype divergence were explored using Principal Coordinate Analysis (PCoA) and Analysis of Molecular Variance (AMOVA) in GenAlEx v6.51 (Peakall & Smouse 2012). Median-joining haplotype networks were constructed using NETWORK v10.1, and pairwise Fst values were estimated with DnaSP v6 (Rozas *et al.* 2017).

## RESULTS AND DISCUSSION

This study provides the first genetic assessment of genetic diversity, phylogenetic relationships, and population structure of *Periophthalmus argentilineatus* from the West Coast of Bengkulu using mitochondrial *COI* sequences. All thirty samples were successfully amplified, producing a 660 bp fragment (Fig. 3). After trimming low-quality regions and aligning sequences, a final consensus fragment of 630 bp was used for all downstream analyses.

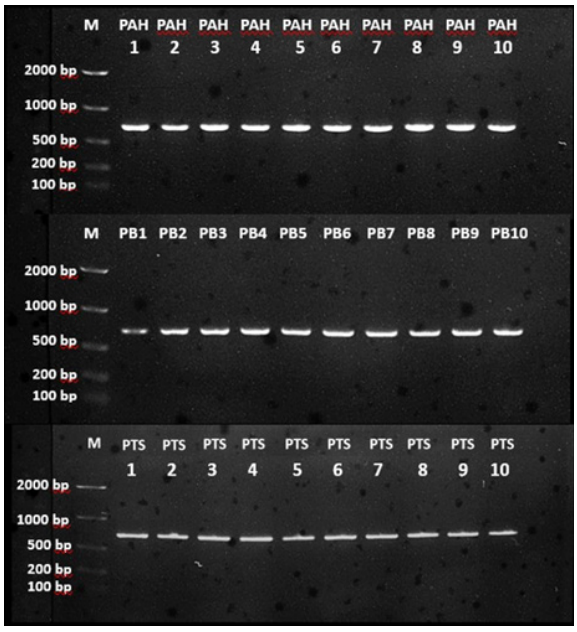


Figure 3 Visualization of *COI* mitochondrial gene amplification in mudskipper (*Periophthalmus argentilineatus*)
Notes: PAH = Air Hitam Coast; PB = Baai Mangrove Forest; PTS = Teluk Sepang Coast; M represents the ladder marker (Bioline).

Species identification was confirmed using BLAST and BOLD analyses, which showed that all specimens correspond to *Periophthalmus argentilineatus* with 99.70 – 100% similarity and 100% query coverage (Table 1). According to Gaffar (2020), a high level of species similarity is typically indicated by query coverage approaching 100%, an e-value close to 0, and identity values nearing 100%.

In addition to confirming species identity, phylogenetic reconstruction and genetic distance estimation were conducted to further examine relationships and clustering patterns among individuals. Additional *COI* sequences of mudskippers from other regions in Indonesia were retrieved from GenBank for comparison. Phylogenetic analyses using Neighbor-Joining (NJ), Maximum Likelihood (ML), and Bayesian Inference (BI) produced congruent topologies (Fig. 4).

All Bengkulu samples clustered within a single lineage corresponding to Clade C previously reported from southern Java (Arisuryanti *et al.* 2024). Clades A and B, which were documented from other Indonesian localities in that study, were not detected in the present dataset. The Bengkulu lineage was strongly supported (NJ and ML bootstrap values = 99%; BI posterior probability = 0.99), indicating robust confidence in the inferred topology. The exclusive detection of Clade C suggests that this lineage extends along the western Indonesian coastline, encompassing southern Java and the West Coast of Bengkulu. The absence of Clades A and B in Bengkulu may reflect broader geographic structuring at the national scale, although expanded sampling across Sumatra is necessary to more clearly delineate lineage boundaries.

Genetic distances among populations (0.00 – 0.80%) further support the close relatedness of individuals within this region (Table 2), consistent with intraspecific variation typically observed in Oxudercidae. Nucleotide composition, with elevated A + T content (56.90%), also conforms to common patterns in mitochondrial genomes of teleost fishes (Table 3).

Table 1 Percentages of identity and query cover of the analyzed mudskipper samples

| No. | Sample code | Percentage of identity | Percentage of query cover | Accession number | Location | Species identification |
|---|---|---|---|---|---|---|
| 1 | PAH1 | 99.85 | 100 | OQ804360 | Pasir Mendit | *P. argentilineatus* |
| 2 | PAH2 | 99.85 | 100 | OQ804360 | Pasir Mendit | *P. argentilineatus* |
| 3 | PAH3 | 100 | 100 | OQ804360 | Pasir Mendit | *P. argentilineatus* |
| 4 | PAH4 | 99.85 | 100 | KU692745 | Pandeglang | *P. argentilineatus* |
| 5 | PAH5 | 100 | 100 | OQ804360 | Pasir Mendit | *P. argentilineatus* |
| 6 | PAH6 | 99.85 | 100 | OQ804360 | Pasir Mendit | *P. argentilineatus* |
| 7 | PAH7 | 99.85 | 100 | OQ804360 | Pasir Mendit | *P. argentilineatus* |
| 8 | PAH8 | 99.85 | 100 | OQ804360 | Pasir Mendit | *P. argentilineatus* |
| 9 | PAH9 | 99.85 | 100 | OQ804360 | Pasir Mendit | *P. argentilineatus* |
| 10 | PAH10 | 99.85 | 100 | OQ804360 | Pasir Mendit | *P. argentilineatus* |
| 11 | PB1 | 99.85 | 100 | OQ804360 | Pasir Mendit | *P. argentilineatus* |
| 12 | PB2 | 100 | 100 | OQ804360 | Pasir Mendit | *P. argentilineatus* |
| 13 | PB3 | 99.85 | 100 | OQ804360 | Pasir Mendit | *P. argentilineatus* |
| 14 | PB4 | 99.85 | 100 | OQ804360 | Pasir Mendit | *P. argentilineatus* |
| 15 | PB5 | 99.85 | 100 | OQ804360 | Pasir Mendit | *P. argentilineatus* |
| 16 | PB6 | 99.85 | 100 | OQ804360 | Pasir Mendit | *P. argentilineatus* |
| 17 | PB7 | 99.70 | 100 | OQ804360 | Pasir Mendit | *P. argentilineatus* |
| 18 | PB8 | 99.70 | 100 | OQ804360 | Pasir Mendit | *P. argentilineatus* |
| 19 | PB9 | 99.85 | 100 | OQ804360 | Pasir Mendit | *P. argentilineatus* |
| 20 | PB10 | 99.85 | 100 | OQ804360 | Pasir Mendit | *P. argentilineatus* |
| 21 | PTS1 | 99.85 | 100 | OQ804360 | Pasir Mendit | *P. argentilineatus* |
| 22 | PTS2 | 100 | 100 | OQ804360 | Pasir Mendit | *P. argentilineatus* |
| 23 | PTS3 | 99.85 | 100 | OQ804360 | Pasir Mendit | *P. argentilineatus* |
| 24 | PTS4 | 99.70 | 100 | OQ804360 | Pasir Mendit | *P. argentilineatus* |
| 25 | PTS5 | 99.85 | 100 | OQ804360 | Pasir Mendit | *P. argentilineatus* |
| 26 | PTS6 | 100 | 100 | OQ804360 | Pasir Mendit | *P. argentilineatus* |
| 27 | PTS7 | 100 | 100 | OQ804360 | Pasir Mendit | *P. argentilineatus* |
| 28 | PTS8 | 99.85 | 100 | OQ804360 | Pasir Mendit | *P. argentilineatus* |
| 29 | PTS9 | 100 | 100 | OQ804360 | Pasir Mendit | *P. argentilineatus* |
| 30 | PTS10 | 99.85 | 100 | OQ804360 | Pasir Mendit | *P. argentilineatus* |

Notes: PAH = Air Hitam Coast; PB = Baai Mangrove Forest; PTS = Teluk Sepang Coast.

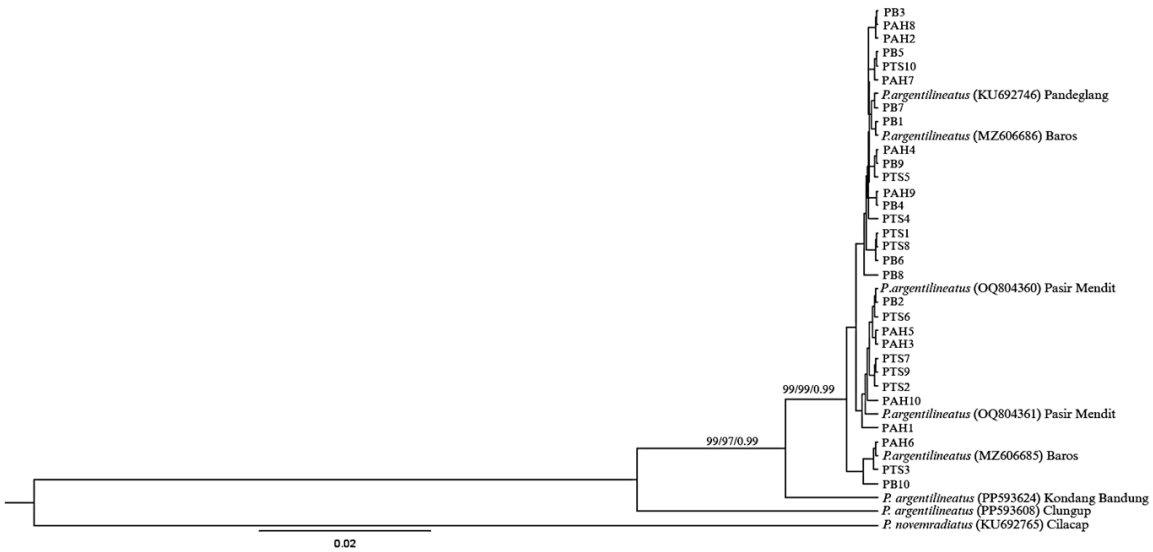


Figure 4 Phylogenetic tree of *Periophthalmus argentilineatus* based on topologies generated using Neighbor Joining (NJ), Maximum Likelihood (ML), and Bayesian Inference (BI)

Notes: Values at the nodes represent NJ/ML bootstrap support and BI posterior probability, respectively PAH = Air Hitam Coast; PB = Baai Mangrove Forest; PTS = Teluk Sepang Coast.

Table 2 Percentage of mitochondrial *COI* genetic distances of *Periophthalmus argentilineatus* from the West Coast of Bengkulu

| | PAH | PB | PTS |
|---|---|---|---|
| **PAH** | 0.18 (0.00 – 0.32) | | |
| **PB** | 0.20 (0.00 – 0.64) | 0.22 (0.00 – 0.80) | |
| **PTS** | 0.16 (0.00 – 0.48) | 0.19 (0.00 – 0.80) | 0.15 (0.00 – 0.32) |

Notes: PAH = Air Hitam Coast; PB = Baai Mangrove Forest; PTS = Teluk Sepang Coast.

Table 3 Nucleotide composition of *P. argentilineatus* from the three studied populations

| | T(U) | C | A | G | A + T | G + C |
|---|---|---|---|---|---|---|
| **PAH** | 31.21 | 25.78 | 25.71 | 17.30 | 56.92 | 43.08 |
| **PB** | 31.14 | 25.84 | 25.70 | 17.32 | 56.84 | 43.16 |
| **PTS** | 31.22 | 25.76 | 25.71 | 17.30 | 56.94 | 43.06 |

Notes: PAH = Air Hitam Coast; PB = Baai Mangrove Forest; PTS = Teluk Sepang Coast. T(U) = Thymine (Uracil); C = Cytosine; A = Adenine; G = Guanine; A + T = Adenine + Thymine; G + C = Guanine + Cytosine.

The comparison of nucleotide proportions among the three populations revealed a consistently high A + T content (56.8 – 56.9%) relative to G + C content (43.0 – 43.1%), with nucleotide differences across T, C, A, and G ranging only from 0 – 0.1%. This A + T predominance is consistent with earlier reports on *Periophthalmus* (Rha'ifa *et al.* 2021; Febrianti *et al.* 2023). Satoh *et al.* (2016) demonstrated that the mitochondrial *COI* gene in fishes exhibits an AT-biased nucleotide composition.

Analysis of the 630 bp *COI* sequences from 30 individuals identified nine variable sites, all of which were transitional mutations detected at nucleotide positions 42, 74, 185, 195, 285, 322, 372, 393, 456, and 516, with two of these sites (372 and 456) being parsimony-informative (Table 4). The high proportion of transitional mutations aligns with the general pattern of nucleotide substitutions, in which same-type base changes occur more frequently because they introduce minimal distortion to the DNA helix and readily arise through deamination (Zou & Zhang 2020).

Translation of the sequences showed that only one of the nine substitutions was nonsynonymous, resulting in an amino acid change from glycine to glutamic acid at codon 65. The predominance of transitional mutations together with the very low level of nonsynonymous substitution indicates that the *COI* gene is under purifying selection, a pattern commonly reported for mitochondrial protein-coding genes. This observation is consistent with the findings of Restrepo-Arias *et al.* (2025), who demonstrated that a higher prevalence of synonymous substitutions generally reflects negative selection acting to maintain the functional integrity of the gene.

Haplotype diversity (h) and nucleotide diversity ($\pi$) are key indicators of genetic variation. A population is considered to have high genetic diversity when Hd > 0.5 or $\pi$ > 0.005 (Grant *et al.* 1998; Luo *et al.* 2023). Analysis of intraspecific genetic variation showed a haplotype diversity (Hd) of 0.708 and a nucleotide diversity ($\pi$) of 0.00182. At the population level (PAH, PB, PTS), a total of nine haplotypes were identified, with five, five, and four haplotypes in each population, respectively. Haplotype diversity ranged from 0.667 to 0.756, while nucleotide diversity remained low ($\pi$ = 0.0015 – 0.0021) (Table 5).

Table 4 Polymorphic sites and amino acids of the mitochondrial *COI* gene of *P. argentilineatus* from the West Coast of Bengkulu

| Codon site | *Haplotype* | 14 | | | 25 | | | 65 | | | 95 | | | 108 | | | 124 | | | 131 | | | 152 | | | 172 | | |
|---|---|---|---|---|---|---|---|---|---|---|---|---|---|---|---|---|---|---|---|---|---|---|---|---|---|---|---|---|
| | | | | | | | | 1 | 1 | 1 | 2 | 2 | 2 | 3 | 3 | 3 | 3 | 3 | 3 | 3 | 3 | 3 | 4 | 4 | 4 | 5 | 5 | 5 |
| Nucleotide site | | 4 | 4 | 4 | 7 | 7 | 7 | 9 | 9 | 9 | 8 | 8 | 8 | 2 | 2 | 2 | 7 | 7 | 7 | 9 | 9 | 9 | 5 | 5 | 5 | 1 | 1 | 1 |
| | | 0 | 1 | 2 | 3 | 4 | 5 | 3 | 4 | 5 | 3 | 4 | 5 | 2 | 3 | 4 | 0 | 1 | 2 | 1 | 2 | 3 | 4 | 5 | 6 | 4 | 5 | 6 |
| PAH1 | H1 | C | G | C | G | G | G | G | C | A | G | A | A | C | T | A | T | T | C | A | T | T | A | T | T | C | T | C |
| PAH2 | H2 | . | | T | . | . | . | . | . | . | . | . | . | . | . | . | . | . | . | . | . | . | . | . | C | . | . | . |
| PAH3 | H3 | . | . | T | . | . | . | . | . | . | . | . | . | . | . | . | . | . | . | . | . | . | . | . | . | . | . | . |
| PAH4 | H2 | . | . | T | . | . | . | . | . | . | . | . | . | . | . | . | . | . | . | . | . | . | . | . | C | . | . | . |
| PAH5 | H3 | . | . | T | . | . | . | . | . | . | . | . | . | . | . | . | . | . | . | . | . | . | . | . | . | . | . | . |
| PAH6 | H4 | . | . | T | . | . | . | . | . | . | . | . | . | . | . | . | . | . | T | . | . | . | . | . | . | . | . | . |
| PAH7 | H2 | . | . | T | . | . | . | . | . | . | . | . | . | . | . | . | . | . | . | . | . | . | . | . | C | . | . | . |
| PAH8 | H2 | . | . | T | . | . | . | . | . | . | . | . | . | . | . | . | . | . | . | . | . | . | . | . | C | . | . | . |
| PAH9 | H2 | . | . | T | . | . | . | . | . | . | . | . | . | . | . | . | . | . | . | . | . | . | . | . | C | . | . | . |
| PAH10 | H5 | . | . | T | . | . | . | . | . | . | . | . | . | T | . | . | . | . | . | . | . | . | . | . | . | . | . | . |
| PB1 | H2 | . | . | T | . | . | . | . | . | . | . | . | . | . | . | . | . | . | . | . | . | . | . | . | C | . | . | . |
| PB2 | H3 | . | . | T | . | . | . | . | . | . | . | . | . | . | . | . | . | . | . | . | . | . | . | . | . | . | . | . |
| PB3 | H2 | . | . | T | . | . | . | . | . | . | . | . | . | . | . | . | . | . | . | . | . | . | . | . | C | . | . | . |
| PB4 | H2 | . | . | T | . | . | . | . | . | . | . | . | . | . | . | . | . | . | . | . | . | . | . | . | C | . | . | . |
| PB5 | H2 | . | . | T | . | . | . | . | . | . | . | . | . | . | . | . | . | . | . | . | . | . | . | . | C | . | . | . |
| PB6 | H2 | . | . | T | . | . | . | . | . | . | . | . | . | . | . | . | . | . | . | . | . | . | . | . | C | . | . | . |
| PB7 | H6 | . | . | T | . | . | . | . | . | . | . | . | . | . | . | . | . | . | . | . | . | C | . | . | C | . | . | . |
| PB8 | H7 | . | . | T | . | . | . | . | . | . | . | . | G | . | . | . | . | . | . | . | . | . | . | . | C | . | . | . |
| PB9 | H2 | . | . | T | . | . | . | . | . | . | . | . | . | . | . | . | . | . | . | . | . | . | . | . | C | . | . | . |
| PB10 | H8 | . | . | T | . | A | . | . | . | G | . | . | . | . | . | . | . | . | T | . | . | . | . | . | . | . | . | . |
| PTS1 | H2 | . | . | T | . | . | . | . | . | . | . | . | . | . | . | . | . | . | . | . | . | . | . | . | C | . | . | . |
| PTS2 | H3 | . | . | T | . | . | . | . | . | . | . | . | . | . | . | . | . | . | . | . | . | . | . | . | . | . | . | . |
| PTS3 | H4 | . | . | T | . | . | . | . | . | . | . | . | . | . | . | . | . | . | T | . | . | . | . | . | . | . | . | . |
| PTS4 | H9 | . | . | T | . | . | . | . | . | . | . | . | . | . | . | . | . | . | . | . | . | . | . | . | C | . | . | T |
| PTS5 | H2 | . | . | T | . | . | . | . | . | . | . | . | . | . | . | . | . | . | . | . | . | . | . | . | C | . | . | . |
| PTS6 | H3 | . | . | T | . | . | . | . | . | . | . | . | . | . | . | . | . | . | . | . | . | . | . | . | . | . | . | . |
| PTS7 | H3 | . | . | T | . | . | . | . | . | . | . | . | . | . | . | . | . | . | . | . | . | . | . | . | . | . | . | . |
| PTS8 | H2 | . | . | T | . | . | . | . | . | . | . | . | . | . | . | . | . | . | . | . | . | . | . | . | C | . | . | . |
| PTS9 | H3 | . | . | T | . | . | . | . | . | . | . | . | . | . | . | . | . | . | . | . | . | . | . | . | . | . | . | . |
| PTS10 | H2 | . | . | T | . | . | . | . | . | . | . | . | . | . | . | . | . | . | . | . | . | . | . | . | C | . | . | . |

| Amino Acid Site - | | 14 | 25 | 65 | 95 | 108 | 124 | 131 | 152 | 172 |
|---|---|---|---|---|---|---|---|---|---|---|
| PAH1 | H1 | . | . | . | . | . | . | . | . | . |
| PAH2 | H2 | . | . | . | . | . | . | . | . | . |
| PAH3 | H3 | . | . | . | . | . | . | . | . | . |
| PAH4 | H2 | . | . | . | . | . | . | . | . | . |
| PAH5 | H3 | . | . | . | . | . | . | . | . | . |
| PAH6 | H4 | . | . | . | . | . | . | . | . | . |
| PAH7 | H2 | . | . | . | . | . | . | . | . | . |
| PAH8 | H2 | | . | | | . | | | . | . |
| PAH9 | H2 | . | . | . | . | . | . | . | . | . |
| PAH10 | H5 | . | . | . | . | . | . | . | . | . |
| PB1 | H2 | | . | | | . | | | . | . |
| PB2 | H3 | . | . | . | . | . | . | . | . | . |
| PB3 | H2 | . | . | . | . | . | . | . | . | . |
| PB4 | H2 | . | . | . | . | . | . | . | . | . |
| PB5 | H2 | . | . | . | . | . | . | . | . | . |
| PB6 | H2 | . | . | . | . | . | . | . | . | . |
| PB7 | H6 | . | . | . | . | . | . | . | . | . |
| PB8 | H7 | . | . | . | . | . | . | . | . | . |
| PB9 | H2 | . | . | . | . | . | . | . | . | . |
| PB10 | H8 | . | . | E | . | . | . | . | . | . |
| PTS1 | H2 | . | . | . | . | . | . | . | . | . |
| PTS2 | H3 | . | . | . | . | . | . | . | . | . |
| PTS3 | H4 | . | . | . | . | . | . | . | . | . |
| PTS4 | H9 | . | . | . | . | . | . | . | . | . |
| PTS5 | H2 | . | . | . | . | . | . | . | . | . |
| PTS6 | H3 | . | . | . | . | . | . | . | . | . |
| PTS7 | H3 | . | . | . | . | . | . | . | . | . |
| PTS8 | H2 | . | . | . | . | . | . | . | . | . |
| PTS9 | H3 | . | . | . | . | . | . | . | . | . |
| PTS10 | H2 | . | . | . | . | . | . | . | . | . |

Notes: PAH = Air Hitam Coast; PB = Baai Mangrove Forest; PTS = Teluk Sepang Coast. T(U) = Thymine (Uracil);
C = Cytosine; A = Adenine; G = Guanine; A + T = Adenine + Thymine; G + C = Guanine + Cytosine;
G = Glycine; E = Glutamic acid; V = Valine; L = Lysine; A = Alanine; T = Threonine.

Moderate haplotype diversity and low nucleotide diversity were also reported in *P. novemradiatus* and *P. kalolo* (Tan *et al.* 2020; Arisuryanti *et al.* 2024). Similar patterns were observed in several other fish species, including the crescent perch (*Terapon jarbua*) (Chanthran *et al.* 2020), longtail tuna (*Thunnus tonggol*) (Kasim *et al.* 2020), and the brushtooth lizardfish (*Saurida undosquamis*) (Tan *et al.* 2022). Tajima's D values were negative for both the total population (D = −1.53530) and individual populations (D = −0.35591 to −1.49289). The combination of moderate haplotype diversity, low nucleotide diversity, and negative Tajima's D values is consistent with a demographic scenario involving historical bottleneck followed by rapid population expansion. Under such a model, new mutations accumulate after expansion, producing multiple closely related haplotypes with low overall sequence divergence. Similar genetic signatures have been documented in other coastal fishes, where demographic fluctuations interact with high dispersal potential.

Population structure analyses indicate low or undetectable genetic differentiation among sampling sites. AMOVA results showed that all observed genetic variation was partitioned within populations (100%), with no detectable variation among populations (0%). The estimated variance component among populations was negligible (0.0%) compared with the within-population estimate of 0.578 (Table 6). Consistently, genetic differentiation (Fst) values ranged from −0.07710 to 0.02072 (Table 7) further supporting high connectivity along the coastline rather than pronounced population subdivision.

Table 5 Genetic variation of *P. argentilineatus* from the West Coast of Bengkulu

| Sample Code | bp | Number of Individual | Number of *Haplotype* | *Variabel sites* | *Parsimony sites* | *Haplotype Diversity* (Hd) | Tajima's D* | *Nucleotide diversity* (π) | ts+tv |
|---|---|---|---|---|---|---|---|---|---|
| PAH | 630 | 10 | 5 | 4 | 1 | 0.756 | -0.70161 | 0.00183 | 4+0 |
| PB | 630 | 10 | 5 | 6 | 1 | 0.667 | -1.49289 | 0.00215 | 6+0 |
| PTS | 630 | 10 | 4 | 3 | 1 | 0.733 | -0.35591 | 0.00152 | 3+0 |
| | 630 | 30 | 9 | 9 | 2 | 0.708 | -1.53530 | 0.00182 | 9+0 |

Table 6 AMOVA analysis of *P. argentilineatus* from the West Coast of Bengkulu based on mitochondrial *COI* gene data

| Source | df | SS | MS | Est.Var | % |
|---|---|---|---|---|---|
| *Among Pops* | 2 | 1.067 | 0.533 | 0.000 | 0% |
| *Within Pops* | 27 | 15.600 | 0.578 | 0.578 | 100% |
| **Total** | **29** | **16.667** | | **0.578** | **100%** |

Table 7 Genetic differentiation among populations of *P. argentilineatus* from the West Coast of Bengkulu based on mitochondrial *COI* gene data

| | PAH | PB | PTS |
|---|---|---|---|
| **PAH** | | | |
| **PB** | 0.01910 | | |
| **PTS** | -0.07710 | 0.02072 | |

Notes: PAH = Air Hitam Coast; PB = Baai Mangrove Forest; PTS = Teluk Sepang Coast.

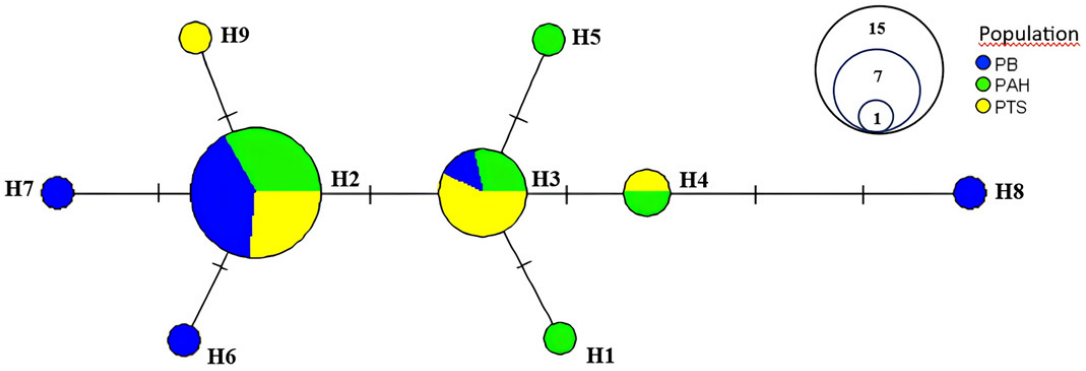


Figure 5 Haplotype network of *P. argentilineatus* samples from the West Coast of Bengkulu based on the mitochondrial *COI* gene

Fish dispersal potential can be markedly affected by oceanographic conditions, which are widely regarded as major determinants of population genetic differentiation (Massimo *et al.* 2009). Environmental characteristics of the Bengkulu coastline likely enhance larval transport. The region is characterized by a shallow coastal profile with a slope of < 1° and depths of only 65 m within 2 nautical miles of shore (Soeprobowati *et al.* 2022). These conditions contribute to extreme low-tide events during the annual tidal cycle, during which the shoreline may recede tens to hundreds of meters. Such extreme tidal retreats can effectively transport larvae from intertidal habitats to more open waters where surface currents are stronger. Comparable findings were reported by Liu *et al.* (2025), who documented horizontal tidal retreat distances reaching up to 26 km on gently sloping coasts. Enhanced water movement during extreme low tides may therefore facilitate long-distance larval dispersal among sampling sites.

Taken together, these factors likely represent key mechanisms underlying the low or undetectable population structure observed in *P. argentilineatus* from the West Coast of Bengkulu. The combination of planktonic larval dispersal, coastal geomorphology, and hydrodynamic processes may facilitate extensive connectivity, leading to shared haplotypes across sites and very low Fst values (Fig.5).

Such substantial gene flow may contribute to demographic stability and potential resilience to localized disturbances. At the same time, these findings underscore the importance of regional-scale oceanographic and ecological processes in shaping genetic patterns in intertidal fish species.

## CONCLUSION

This study demonstrates that *Periophthalmus argentilineatus* populations along the West Coast of Bengkulu exhibit high haplotype diversity but low nucleotide diversity, with no detectable genetic structure among the three sampling sites. Phylogenetic analyses place all individuals within clade C, consistent with previous findings from southern Java, while genetic distance confirm close relatedness within the species. AMOVA and very low $F_{st}$ values indicate complete genetic homogeneity and extensive connectivity among populations. The high level of gene flow is likely facilitated by a planktonic larval phase that enables dispersal across coastal areas. This process is further supported by local oceanographic and geomorphological conditions, including shallow coastal slopes, extreme tidal retreats, and strong surface currents that enhance larval transport. Consequently, *P. argentilineatus* populations in this region function as a genetically cohesive unit, emphasizing the importance of larval dispersal and coastal dynamics in maintaining population connectivity.

## ACKNOWLEDGMENTS

I extend my gratitude to the Head of Laboratory of Genetics and Breeding, Faculty of Biology, Universitas Gadjah Mada, for granting permission to use the research facilities. I also sincerely thank Vestidhia Yunisya Atmaja, S.Si., M.Sc., for her assistance in data analysis, as well as to the local fishermen who helped collect mudskipper samples at the study sites.

## REFERENCES


Abiaobo NO, Asuquo IE, Ejogu IN, James EJ. 2021. Ecology and evolutionary biology aspect of the biology of Periophthalamus barbarous (Mudskipper) from Jaja Creek, Niger Delta, Nigeria. Ecol Evol Biol 6(1):15–22. DOI: 10.11648/j.eeb.20210601.14

Aji KW, Arisuryanti T. 2021. Molecular identification of mudskipper fish (*Periophthalmus* spp.) from Baros Beach, Bantul, Yogyakarta. J Trop Biodivers Biotechnol 6(3):1–13. DOI: 10.22146/jtbb.66391

Arisuryanti T, Aji KW, Herawati H, Sari IP, Rha'ifa FA, Febriyanti D, Priyono DS. 2024. Cryptic diversity of barred mudskippers, *Periophthalmus argentilineatus* (Valenciennes, 1837), from the Southern Coast of Java and East Lombok, Indonesia inferred by *COI* mitochondrial gene. J Trop Biodivers Biotechnol 9(3):jtbb84328. DOI: 10.22146/jtbb.84328

Arisuryanti T, Firdaus NUN, Hakim L. 2020. Genetic characterization of striped snakehead (Channa striata Bloch, 1793) from Arut River, Central Kalimantan inferred from *COI* mitochondrial gene. AIP Conf Proc 2260(1):020001. Yogyakarta (ID): AIP Publishing LLC. DOI: 10.1063/5.0015905

Chanthran SSD, Lim PE, Li Y, Liao TY, Poong SW, Du J, …, Loh K-H. 2020. Genetic diversity and population structure of *Terapon jarbua* (Forskål, 1775) (Teleostei, Terapontidae) in Malaysian Waters. ZooKeys 911:139–160. DOI: 10.3897/zookeys.911.39222

Chen IS, Hong WS, Jang-Liaw NH, Shao KT. 2015. Population genetic structure of *Boleophthalmus* boddarti (Oxudercinae, Gobiidae) in the northwestern Pacific and the South China Sea. Hydrobiologia 762(1):85–98. DOI: 10.1007/s10750-015-2321-0

Corush JB, Lin C-H, Lee H-J, Chen C-A, Shiao J-C, Chou W-H. 2022.

Amphibious mudskipper populations are genetically connected along coastlines but differentiated across water gaps. J Biogeogr 49(3):655–669. DOI: 10.1111/jbi.14345

Darrib D, Taboada GL, Doallo R, Posada D. 2012. jModelTest 2: more models, new heuristics and parallel computing. Nat Methods 9(8):772. DOI: 10.1038/nmeth.2109

Febriyanti D, Aji KW, Priyono DS, Arisuryanti T. 2023. Genetic identification of two mudskipper species (Oxudercidae: *Periophthalmus*) from Kulon Progo, Special Region of Yogyakarta, Indonesia. J Trop Biodivers Biotechnol 8(2):78161. DOI: 10.22146/jtbb.78161

Gaffar S. 2020. Analisis sekuen mtDNA *COI* pari totol biru yang didaratkan di tempat pendaratan ikan Kota Tarakan. [Analysis of mtDNA *COI* sequences of the blue-spotted stingray landed at the fish landing site in Tarakan City]. J Harpodon Borneo 13(2):80–89. DOI: 10.35334/harpodon.v13i2.1835

Grant W, Bowen BW. 1998. Shallow population histories in deep evolutionary lineages of marine fishes: Insights from sardines and anchovies and lessons for conservation. J Hered 89:415–426. DOI: 10.1093/jhered/89.5.415

Hebert PD, Cywinska A, Ball SL, deWaard JR. 2003. Biological identifications through DNA barcodes. Biol Sci 270(1512):313–321. DOI: 10.1098/rspb.2002.2218

Kasim NS, Mat Jaafar TNA, Mat Piah R, Arshaad WM, Mohd Nor SA, Habib A, …, Tan MP. 2020. Recent population expansion of longtail tuna *Thunnus tonggol* (Bleeker, 1851) inferred from the mitochondrial DNA markers. PeerJ 8:e9679. DOI: 10.7717/peerj.9679

Kutschera U, Elliott JM. 2013. Do mudskippers and lungfishes elucidate the early evolution of four-limbed vertebrates?. Evol Educ Outreach 6:1-8. DOI: 10.1186/1936-6434-6-8

Liu Y, Zhang H, Zhang Y, Wang Z. 2025. Dynamics and drivers of tidal flat morphology in China. Nat Commun 16:2153. DOI: 10.1038/s41467-025-57525-4

Luo Y, Zhang Y, Cheng R, Li Q, Zhang Y, Li Y, Shen Y. 2023. Genetic diversity of Jinshaia sinensis (Cypriniformes, Balitoridae) distributed upstream of the Yangtze River. Fishes 8(2):75. DOI: 10.3390/fishes8020075

Lv J, Wu S, Zhang Y, Chen Y, Feng C, Yuan X, …, Lin X. 2014. Assessment of four DNA fragments (*COI*, *16S* rDNA, *ITS2, 12S* rDNA) for species identification of the Ixodida (Acari: Ixodida). Parasit Vectors 7:1–11. DOI: 10.1186/1756-3305-7-93

Maddison WP, Maddison DR. 2019. Mesquite: A Modular System for Evolutionary Analysis. Version 3.6.1. [Internet]. Available from: http://www.mesquiteproject.org

Massimo G, Mario LM, Vincenzo C. 2009. Life style and genetic variation in teleosts: The case of pelagic (Aphia minuta) and benthic (Gobius niger) gobies (perciformes: gobiidae). Mar Biol 156:239–252. DOI: 10.1007/s00227-008-1078-9

Muhala V, Guimarães-Costa A, Bessa-Silva AR, Rabelo LP, Carneiro J, Macate IE, …, Sampaio I. 2024. Comparative mitochondrial genome brings insights to slight variation in gene proportion and large intergenic spacer and phylogenetic relationship of mudskipper species. Sci Rep 14(1):3358. DOI: 10.1038/s41598-024-52979-4

Murdy EO. 1989. A taxonomic revision and cladistic analysis of the oxudercine gobies (Gobiidae: Oxudercinae). Rec Aust Mus Suppl 11:1–93. DOI: 10.3853/j.0812-7387.11.1989.93

Peakall R, Smouse PE. 2012. GenAlEx 6.5: Genetic analysis in Excel. Population genetic software for teaching and research – An update. Bioinformatics 28(19):2537–2539. DOI: 10.1093/bioinformatics/bts460

Polgar G, Sacchetti A, Galli P. 2014. Phylogeography and demographic history of two widespread Indo-Pacific mudskippers (Gobiidae: *Periophthalmus*). Mar Biol 161:1325–1342. DOI: 10.1007/s00227-014-2414-0

Rambaut A. 2019. FigTree v 1.4.4. [Internet]. Available from: http://tree.bio.ed.ac. uk/software/figtree/

Restrepo-Arias MA, Zerpa-Catanho D, Martínez-Méndez N, Pérez-Pérez JE. 2025. Patterns of genetic diversity in five species across genus: A comparative analysis using conserved genes. J King Saud Univ Sci 37:102482. DOI: 10.1016/j.avrs.2025.100279

Rhaifa FA, Audrea DJ, Hakim L, Arisuryanti T. 2021. DNA barcode of barred mudskipper (*Periophthalmus argentilineatus* Valenciennes, 1837) from Tekolok Estuary (West Nusa Tenggara, Indonesia) and their phylogenetic relationship with other indonesian barred mudskippers. J Trop Biodivers Biotechnol 6(2):jtbb59702. DOI: 10.22146/jtbb.59702

Rozas J, Rerrer-Matta A, Sanchez-DelBarrio JC, Guirao-Rico S, Librado P, Ramos Onsins SE, Sanchez-Garcia A. 2017. DNA SP 6: DNA sequence polymorphism analysis of large data sets. Mol Biol Evol 13(12):3299–3302. DOI: 10.1093/molbev/msx248

Rumisha C, Ulotu ET, Mlay RM. 2024. Unveiling genetic diversity and connectivity of mudskippers in MPAs and NPAs along the Tanzanian Coastline. Reg Stud Mar Sci 77:103538. DOI: 10.1016/j.rsma.2023.103538

Satoh TP, Miya M, Mabuchi K, Nishida M. 2016. Structure and variation of mitochondrial genome of fishes. BMC Genomics 17:719. DOI: 10.186/s12864-016-3054-y

Shabrina FN, Wibowo K, Arisuryanti T. 2024. Cryptic diversity of mudskipper genus *Boleophthalmus* (Gobiiformes: Oxudercidae) from the north coast of East Java, Indonesia. Biodiversitas 25(1):412–420. DOI: 10.13057/biodiv/d250148

Soeprobowati TR, Aini N, Fitri M, Suwondo S. 2022. Species composition and distribution in the mangrove ecosystem in the City of Bengkulu. Water 14(22):3516. DOI: 10.3390/w14223516

Suchard MA, Lemey P, Baele G, Ayres DL, Drummond AJ, Rambaut A. 2018. Bayesian phylogenetic and phylodynamic data integration using BEAST 1.10. Virus Evol. 4:1–5. DOI: 10.1093/ve/vey016

Sunarni S, Maturbongs MR. 2016. Biodiversitas dan kelimpahan ikan gelodok (mudskipper) di daerah intertidal Pantai Payumb, Merauke [Biodiversity and abundance of mudskipper fish in the intertidal zone of Payumb Beach, Merauke]. Proceedings: National Seminar on Maritime Affairs and Small Islands Resources 1(1):125–131. Ternate (ID): Universitas Khairun.

Tamura K, Stecher G, Kumar S. 2021. MEGA11: Molecular Evolutionary Genetic Analysis Version 11. Mol Biol Evol 38(7):3022–3027. DOI: 10.1093/molbev/msab120

Tan MP, Gan HM, Nabilsyafiq MH, Mazlan AG, Mat Jaafar TNA, SitiAzizah MN, …, Sung YY. 2020. Genetic diversity of the Pearse's mudskipper *Periophthalmus* novemradiatus (Perciformes: Gobiidae) and characterization of its complete mitochondrial genome. Thalassas Int J Mar Sci 36:103–113. DOI: 10.1007/s41208-019-00189-5

Tan MP, Sammogam R, Mohd Nur NF, Mohd Yusoff NIS, Mat Jaafar TNA, Mohd Nor SA, …, Megarajan S. 2022. Genetic polymorphism and phylogenetic relationships of the brushtooth lizardfish (*Saurida undosquamis*) based on mitochondrial DNA markers. Mar Biodivers 52:13. DOI: 10.1007/s12526-021-01250-4

Thacker CE. 2003. Molecular phylogeny of the gobioid fishes (Teleostei: Perciformes: Gobioidei). Mol Phylogenet Evol 26(3):354–368. DOI: 10.1016/S1055-7903(02)00361-5

Ward RD, Zemlak TS, Innes BH, Last PR, Hebert PDN. 2005. DNA barcoding Australia's fish species. Philos Trans R Soc B Biol Sci 360(1462):1847–1857. DOI: 10.1098/rstb.2005.1716

Zhang Q, Hong W, Dai Q, Zhang J, Cai Y, Huang J. 1989. Studies on induced ovulation, embryonic development and larval rearing of the mudskipper (*Boleophthalmus* pectinirostris). Aquaculture 83:375–385. DOI: 10.1016/0044-8486(89)90048-3

Zou Z, Zhang J. 2020. Are synonymous mutations selectively neutral? Mol Biol Evol 37(1):1–8. DOI: 10.1093/molbev/msaa200